

# **Weak measurement, projective measurement and quantum-to-classical transitions in electron-photon interactions**

Yiming Pan<sup>1†</sup>, Eliahu Cohen<sup>2†</sup>, Ebrahim Karimi<sup>3</sup>, Avraham Gover<sup>4</sup>, Ido Kaminer<sup>5</sup> and Yakir Aharonov<sup>6,7</sup>

1. Department of Physics of Complex Systems, Weizmann Institute of Science, Rehovot 7610001, Israel
2. Faculty of Engineering and the Institute of Nanotechnology and Advanced Materials, Bar Ilan University, Ramat Gan 5290002, Israel
3. Department of Physics, University of Ottawa, Ottawa, Ontario, K1N 6N5, Canada
4. Department of Electrical Engineering Physical Electronics, Tel Aviv University, Ramat Aviv 6997801, Israel
5. Department of Electrical Engineering, Technion: Israel Institute of Technology, Haifa 3200003, Israel
6. School of Physics and Astronomy, Tel Aviv University, Ramat Aviv 6997801, Israel
7. Institute for Quantum Studies, Chapman University, Orange, CA 92866, USA

†Correspondence and requests for materials should be addressed to E.C. (eliahu.cohen@biu.ac.il) and Y.P. (yiming.pan@weizmann.ac.il).

## **Abstract**

How does the quantum-to-classical transition of measurement occur? This question is vital for both foundations and applications of quantum mechanics. We present a full characterization of classical and quantum electron-photon interactions employing a measurement-based framework. To explain the emergence of ‘classicality’ in the measurement process, we first analyze the transition from projective measurement to weak measurement in generic light-matter interactions. We then show that any classical electron-laser interaction can be represented as an outcome of a weak measurement. In particular, the appearance of classical point-particle acceleration is an example of an amplified weak value resulting from weak measurement. We quantify both measurement regimes with a universal factor  $\exp(-\Gamma^2/2)$ , characterizing the measurement transition from quantum to classical, where  $\Gamma$  corresponds to the ratio between the electron wavepacket size and the optical wavelength. Our analysis of the transition from projective to weak measurement reveals the quantum-to-classical transition in electrodynamics, enabling to employ the very essence of wave-particle duality in quantum measurement.

Measurement lies at the heart of quantum mechanics. It allows us to probe the system of interest through a measuring pointer coupled to its observables. The interaction between the quantum system and quantum pointer is later classically amplified for the outcome to be seen macroscopically. However, in the context of light-matter interactions, sometimes either the measured system or measuring pointer (or both) can be treated classically. These interactions are usually modelled by classical or quantum electrodynamics, with a wealth of widely explored effects and experimental schemes such as photon-induced near-field electron microscopy (PINEM) [1,2] or dielectric laser accelerators (DLA) [3,4], both inspiring our current exploration. We argue that there is a continuous transition between classical and quantum interactions between electrons and photons, which we would like to analyze when examining several limiting cases of the measurement process.

We wish to investigate the possible outcomes when electrons and photons are coupled, to classify in which cases they can be regarded as ‘classical’ or ‘quantum’ measuring pointers. In particular, we study the transition process between the two regimes. In light of current experimental capabilities of manipulating electrons and photons, the quantitative wave-particle duality of electrons and also the quantum-to-classical transitions of photons are both controllable in ultra-fast transmission electron microscopy (UTEM) [1,2] and in quantum light preparation [5], respectively. In the wavepacket representation with electron wavepacket size ( $\Delta_z$ ), the point-particle-like picture of free electrons can be defined in the limit  $\Delta_z \rightarrow 0$ , and, conversely, the plane-wave-like picture in the opposite limit  $\Delta_z \rightarrow \infty$ . Similarly, the photon state holds its own quantum-to-classical transition. For concreteness, the single-photon-added coherent state plays a key role in the range between a coherent state (‘classical’) and a single Fock number state (‘quantum’) [5,6]. We thus define a parameterized photon state as the basis for possible investigation of the fuzzy border that may separate ‘quantum’ from ‘classical’ measurements in the above sense, utilizing the coupling with a single free-electron wavepacket as a measuring pointer.

To be specific, we define the ‘particle-to-wave’ electron state using a Gaussian wavepacket and the ‘quantum-to-classical’ photon state using the representation of a photon-added coherent state. The initially prepared electron and photon states are then respectively given by

$$\begin{aligned} |\Psi\rangle &= \int dp c_p^{(0)} |p\rangle, \\ |\alpha, \nu\rangle &= \frac{\hat{a}^{\dagger \nu} |\alpha\rangle}{\sqrt{\nu! L_\nu(-|\alpha|^2)}}, \end{aligned} \quad (1)$$

where the normalized Gaussian component is  $c_p^{(0)} = (2\pi\sigma_{p_0}^2)^{-1/4} \exp\left(-\frac{(p-p_0)^2}{4\tilde{\Delta}_p^2(t_D)}\right) e^{i(p_0 L_D - E_0 t_D)/\hbar}$  with  $\tilde{\Delta}_p^2(t_D) = \Delta_{p_0}^2 (1 + i\xi t_D)^{-1}$  the chirped momentum uncertainty with chirp factor  $\xi = 2\Delta_{p_0}^2 / m^* \hbar$ ,  $L_D = v_0 t_D$  the pre-interaction draft length with propagation duration  $t_D$ , and  $m^*, v_0, p_0, E_0$  the effective electron mass, the velocity, the average momentum and energy, respectively. Note that the electron wavepacket is only defined in longitudinal dimension (1D), where the electron’s initial momentum distribution is readily obtained as  $\rho^{(0)}(p) = |c_p^{(0)}|^2 = (2\pi\Delta_{p_0}^2)^{-1/2} \exp\left(-\frac{(p-p_0)^2}{2\Delta_{p_0}^2}\right)$ . The photon-added coherent state reduces to the limit of Fock or coherent state for the parameters  $\alpha \rightarrow 0$  or  $\nu \rightarrow 0$ , respectively, with  $L_\nu$  being the Laguerre polynomial of (integer) order  $\nu$  and all other photon indices are suppressed for simplicity. Such photon state was theoretically proposed by Agarwal and Tara [6] and later experimentally realized by Zavatta *et al.* [5]. Following the standard procedure of measurement proposed by von Neumann [7], we can study the quantum-to-classical transitions of measurement of electron-photon coupling as a testing platform of the system-pointer measurement schemes by classifying it into four types of interaction, as shown in Figs. 1b-e: (I) the classical point-particle electron coupling with ‘classical’ photon coherent state; (II) the classical point-particle electron coupling with ‘quantum’ photon Fock state; (III) the quantum plane-wave electron coupling with classical photon; (IV) the quantum plane-wave electron coupling with quantum photon.

Next, without loss of generality, we assume that the coupling interaction between the classical electron ( $\Delta_{z_0} = \hbar/2\Delta_{p_0} \rightarrow 0$ ) and the classical photon ( $v \rightarrow 0, \alpha \neq 0$ ) can be simplified into the canonical Hamilton equations  $\dot{z} = p/m, \dot{p} = -eE_c \cos(\omega t - q_z z(t) + \phi_0)$ , which describe a charged point-particle (-e) moving in the presence of a monochromatic travelling electromagnetic field (laser, microwave field, etc.) with electric component  $E = E_c \cos(\omega t - q_z z + \phi_0)$  having the optical frequency  $\omega$  and the z component of the wave vector  $q_z$  along the propagation direction. With the short timescale approximation  $\dot{z} \approx v_0, z(t) = v_0 t$ , the classical momentum transfer can be thus reduced to  $\Delta p_{\text{point}} = -eE_c \int_0^{L/v_0} \cos(\omega t - q_z(v_0 t) + \phi_0) dt = -\left(\frac{eE_c L}{v_0}\right) \text{sinc}\left(\frac{\bar{\theta}}{2}\right) \cos\left(\frac{\bar{\theta}}{2} + \phi_0\right)$ , in which the synchronization condition is  $\bar{\theta} = (\omega/v_0 - q_z)L$ ,  $L$  is the interaction length and  $v_0$  is the initial velocity of the electron. This is the well-known linear acceleration formula in classical accelerator physics, as well as in the inverse Smith-Purcell effect, or the Dielectric Laser accelerator (DLA) (accelerator on a chirp) [3,4].

This classical acceleration formula offers a hint how to quantum-mechanically measure the electromagnetic field operators (e.g., the vector potential  $\mathbf{A}$ ) via a moving electron wavepacket as a measuring pointer coupled to the measured photonic system. It will be shown how to calculate the classical particle acceleration within the von Neumann measurement scheme [7], as a result of the electron-photon coupling. From the perspective of weak measurement [8], we will see below that the momentum transfer of the pointer after interaction corresponds to the weak value of the vector potential ( $\mathbf{A}$ ) of the photonic system. This applies in the configuration of classical electron pointer coupled to a classical photon system (Fig. 1b). In the other three configurations, the electron-photon couplings indicate a quantum (strong) projective measurement. As a result, the system-pointer measurement inevitably falls into the ‘strong’ category involving a significant momentum change with a subsequent ‘wavefunction collapse’, regardless of whether the electron or photon state corresponds to the quantum limit. This will indicate below how quantum weak measurement can lead to the classical acceleration, thereby possibly implying in general how classical electrodynamics may emerge from a quantum analysis.

Additionally, in the transition from weak to projective measurements, we notice that the identities of electron and photon are reciprocal in the following sense: which is the system or which is the pointer depends on the detection and post-selection configuration of electrons and photons. This underlying reciprocity leads to the system-pointer duality that will be discussed towards the end of this work.

**The quantum-to-classical measurement scheme.** Our analysis of measurement is based on the first order perturbative solution of the ‘relativistically modified’ Schrödinger equation [9-11] for a free electron wavefunction and a quantized radiation field. Following the standard QED treatment, we expand the initial wavefunction in terms of the quantum continuous numbers  $p$  of the electron state and the Fock number-occupation state of the photon, which is given by

$|i\rangle = \sum_{p,\nu} c_{p,\nu}^{(0)} e^{-iE_p t/\hbar} |p,\nu\rangle$ , where  $c_{p,\nu}^{(0)}$  is the component of the combined electron and photon state

$|p,\nu\rangle$  as given in Eq. (1) and  $E_p = c\sqrt{m^2 c^2 + p^2}$ . First order time-dependent perturbation analysis

of the Schrödinger equation results in  $i\hbar \dot{c}_{p',\nu'}^{(1)} = \sum_{p,\nu} c_{p,\nu}^{(0)} \langle p',\nu' | H_I(t) | p,\nu \rangle e^{-i(E_p - E_{p'})t/\hbar}$  and the

interaction Hamiltonian is taken to be  $\hat{H}_I(t) = -e\hat{\mathbf{A}} \cdot \mathbf{p}/\gamma_0 m$  (see the SM file). By integrating in the time domain to infinity, the emission and absorption processes of the first order perturbed coefficients are given by [9] as follows,

$$c_{p',\nu'}^{(1)} = c_{p',\nu'}^{(1)(e)} + c_{p',\nu'}^{(1)(a)}, c_{p',\nu'}^{(1)(e,a)} = \frac{\pi}{2i\hbar} \sum_{p,\nu} c_{p,\nu}^{(0)} \langle p',\nu' | H_I^{(e,a)} | p,\nu \rangle \delta(E_p - E_{p'} \mp \hbar\omega/2\hbar),$$

where the matrix elements  $H_I^{(e,a)}$  correspond to the emission (e) and absorption (a) parts of the interaction Hamiltonian, respectively.

For energy/momentum transfer in electron energy loss spectrum (EELS), the wavepacket acceleration as the pointer shift is thus obtained as  $\Delta E = \sum_{p,\nu} |c_{p,\nu}^{(0)} + c_{p,\nu}^{(1)(e)} + c_{p,\nu}^{(1)(a)}|^2 (E_p - E_0)$ , where

the initial electron energy  $E_0 = \sum_{p,\nu} |c_{p,\nu}^{(0)}|^2 E_p$ . Note that the unnormalized final state

$c_{p,\nu}^{(f)} = c_{p,\nu}^{(0)} + c_{p,\nu}^{(1)(e)} + c_{p,\nu}^{(1)(a)}$  has the photon-emitted (e) and photon-absorbed (a) contribution from

electron-photon scattering processes  $|p, \nu \mp 1\rangle \Rightarrow |p \mp \frac{\hbar\omega}{v_0}, \nu\rangle$  respectively. Here we expand together the expressions comprising  $\Delta E$ , then cancel the initial terms and rewrite as two separate terms:

$$\Delta E^{(1)} = 2 \sum_{p,\nu} \Re \{ \mathbf{c}_{p,\nu}^{(0)*} \cdot \mathbf{c}_{p,\nu}^{(1)(e)} + \mathbf{c}_{p,\nu}^{(0)*} \cdot \mathbf{c}_{p,\nu}^{(1)(a)} \} (E_p - E_0) \quad \text{and} \quad \Delta E^{(2)} = \sum_{p,\nu} \left| \mathbf{c}_{p,\nu}^{(1)(e)} + \mathbf{c}_{p,\nu}^{(1)(a)} \right|^2 (E_p - E_0),$$

where  $\Re$  stands for the real part of the argument. The phase-independent term  $\Delta E^{(2)}$  is the term that corresponds to photon emission rate, as derived from the Fermi's Golden Rule (FGR) [10-12], while the phase-dependent term  $\Delta E^{(1)}$  that originates from quantum interference between the initial state and scattered state is an additional contribution which is usually omitted in the formulation of FGR but leads to the classical linear acceleration [10].

**Classical photon in a coherent state.** In our quantum treatment of the initial electron-photon state as given by  $c_{p,\nu}^{(0)} = c_p^{(0)} c_\nu^{(0)}$ , we consider the initial electron wavepacket of the chirped Gaussian distribution (Eq. 1) combined with a coherent photon state, where  $\nu_0 = \langle \sqrt{\nu_0} | \hat{a}_{\nu_q}^* \hat{a}_{\nu_q} | \sqrt{\nu_0} \rangle = \sum_\nu \nu |c_\nu^{(0)}|^2$  is the total photon number. Substituting into the wavepacket acceleration formula ( $\Delta E$ ) as we derived in previous section, one can obtain the explicit energy transfer with two parts ( $\Delta E = \Delta E^{(1)} + \Delta E^{(2)}$ ) [10]:

$$\begin{aligned} \Delta E^{(1)} &= - (eE_c L) e^{-\Gamma^2/2} \text{sinc} \left( \frac{\bar{\theta}}{2} \right) \cos \left( \frac{\bar{\theta}}{2} + \phi_0 \right) \\ \Delta E^{(2)} &= - \tilde{\Upsilon}^2 \hbar \omega \text{sinc}^2 \left( \frac{\bar{\theta}}{2} \right), \end{aligned} \tag{2}$$

where the normalized photon exchange coefficient is defined as  $\tilde{\Upsilon} = e\tilde{E}_q L / 4\hbar\omega$ . Note that the relation  $\langle \sqrt{\nu_0} | \hat{a}_{\nu_q} | \sqrt{\nu_0} \rangle = \sqrt{\nu_0}$  is taken for the coherent state. A significant pointer-specific extinction parameter  $e^{-\Gamma^2/2}$  was found in the phase dependent energy transfer (2), with a decay parameter given by

$$\Gamma = \left( \frac{\omega}{v_0} \right) \Delta_z(t_D) = \left( \frac{\hbar\omega}{v_0} \right) \frac{\sqrt{1 + \xi^2 t_D^2}}{2\Delta_{p_0}} = \Gamma_0 \sqrt{1 + \xi^2 t_D^2}, \tag{3}$$

with  $\Gamma_0 = \frac{2\pi}{\beta} \left( \frac{\Delta_{z_0}}{\lambda} \right)$ . The extinction parameter ( $e^{-\Gamma^2/2}$ ) demonstrates that the prior history

dependent wavepacket size of a free electron wavepacket as the measuring pointer have physical effects in its interaction with coherent light.

Now, we are able to discuss quantitatively the classical point-particle and quantum plane-wave limits of electron wavepacket acceleration in the interaction with quantized photon state of light as shown in Figs. 1b,d. The particle-to-wave transition of the electron-photon interaction in measuring electron energy loss spectroscopy (EELS) is shown in Fig. 2a. The appearance of ‘classicality’ corresponds to the condition  $e^{-\Gamma^2/2} \rightarrow 1$ , which means that the photon distribution becomes a coherent state describing the ‘classical’ electromagnetic field, and similarly, the electron wavefunction looks like a point-like particle with wavepacket size comparable to the wavelength:  $\Delta_z(t) \ll \beta\lambda$ . Indeed, the wavepacket-dependent acceleration when the wavepacket size is comparable to the wavelength is given by  $\Delta E = \Delta E_{\text{point}} e^{-\Gamma^2/2}$ . The decay parameter ( $\Gamma$ ) implies the measurability of the electron wavepacket size near the classical particle-like regime. On the other hand, the plane-wave limit can be directly defined in the case  $\Delta E^{(1)} \rightarrow 0$ , and it only has the contribution of phase-independent terms. Even in the classical limit, the phase-independent term ( $\Delta E^{(2)}$ ) still has a non-vanishing noise contribution in the form of vacuum fluctuations. This phase-independent term ( $\Delta E^{(2)}$ ) relates to the vacuum expectation value, which acts as quantum noise of spontaneous fluctuation in our electron-photon coupling measurements [10]. Therefore, the phase-dependent term ( $\Delta E^{(1)}$ ) reduces to the classical particle acceleration, but is measurable only if the spontaneous vacuum fluctuation is negligible:  $\Delta E^{(1)} \gg \Delta E^{(2)}$  under  $\nu_0 \gg 1$ .

**Quantum photon in a Fock state.** In contrast, the single Fock state of light corresponds to the photon-added coherent state (Eq. 1), obeying the condition  $\alpha \rightarrow 0$ , i.e.,  $c_v^{(0)} = \delta_{v,\nu_0}$ . When inspecting the wavepacket acceleration expression, it appears that similarly to the case of spontaneous emission, there is no Fock-state stimulated energy transfer due to the orthogonal relations  $\langle \nu_0 | \hat{a}_{\nu_q} | \nu_0 \rangle = \langle \nu_0 | \hat{a}_{\nu_q}^\dagger | \nu_0 \rangle = 0$ . Therefore, one obtains the total energy transfer,

$\Delta E^{(1)} = 0, \Delta E^{(2)} = -\tilde{\Upsilon}^2 \hbar \omega \text{sinc}^2\left(\frac{\bar{\theta}}{2}\right)$ . There is no stimulated radiative interaction as a result of the coupling to the quantum light (radiation wave) in Figs. 1c,e. However, this is not very surprising since the initial single Fock state ( $|\nu_0\rangle$ ) is orthogonal to the emitted and absorbed photon state ( $|\nu_0 \pm 1\rangle$ ), so that the phase-dependent interference term has no contribution. Besides, the second term ( $\Delta E^{(2)}$ ) still produces the wavepacket-independent spontaneous vacuum fluctuation as the inevitable quantum noise in the observation of EELS, the same as in the coherent state representation of light (Eq. 2).

**Weak measurement versus projective measurement.** Let us deepen now to the EELS observation of final electron wavefunction after the interaction. When a quantum electron pointer is coupled to the photon system, the photon-induced outgoing electron momentum distribution is then given by  $\rho^{(f)}(\mathbf{p}) = \sum_{\nu} |c_{p,\nu}^{(0)} + c_{p,\nu}^{(1)(e)} + c_{p,\nu}^{(1)(a)}|^2$ . We find the typical measurement pictures in the two aforementioned limits.

First, in the point-particle limit  $\Delta_{z_0} < \beta\lambda$  (we set  $t_D = 0$  for simplicity) [10, 13], in which case necessarily the initial momentum distribution exceeds the quantum recoil  $\Delta_{p_0} > \hbar\omega/v_0$ , then the final momentum distribution after interaction with the classical photon is:  $\rho_C^{(f)}(\mathbf{p}) = \rho^{(0)}(\mathbf{p} - \Delta\mathbf{p}^{(1)})$ , where the momentum shift is  $\Delta\mathbf{p}^{(1)} = \Delta\mathbf{p}_{\text{point}} e^{-\Gamma^2/2}$  (also corresponding to  $\Delta E^{(1)}$  in Eq. 2). As shown in Figs. 2b,c, the emission and absorption terms overlap with the initial wavepacket momentum distribution and contribute the asymmetrical interference effects with opposite sign, which leads to the momentum shift in the classical point-particle regime. The final momentum distribution of the electron pointer is then reshaped, displaying net momentum shift of small acceleration, as shown in Figs. 2b,c, where we ignore the spontaneous term in the weak-field coupling  $eE_c L/\hbar\omega < 1$ . Except for the universal transition factor  $e^{-\Gamma^2/2}$ , the acceleration/deceleration of the electron wavepacket depends on the synchronism detuning parameter  $\bar{\theta}$  and the relative phase  $\phi_0$ , similar to a charged point-particle moving in the presence

of a classical electromagnetic field ( $\Delta\mathbf{p}_{\text{point}}$ ) in the classical limit ( $\Gamma \rightarrow 0$ ) of interaction between ‘particle-like’ electron and ‘classical’ photon (Fig. 1b). This interaction picture of electron-photon coupling leads to the classical measurement or classical electrodynamics, and also to the weak measurement as displayed in Fig. 2b.

Next, in the plane-wave limit  $\Delta z_0 > \beta\lambda$  (i.e., the criterion of projective measurement), the interference term vanishes and the scattered component dominates, resulting in a final PINEM-kind spectrum of the momentum distribution, as shown in Figs. 2d,e:

$$\rho_Q^{(f)}(\mathbf{p}) = \left(1 - 2\Upsilon^2 \text{sinc}^2\left(\frac{\bar{\theta}}{2}\right)\right) \rho^{(0)}(\mathbf{p}) + \Upsilon^2 \text{sinc}^2\left(\frac{\bar{\theta}}{2}\right) \left( \rho^{(0)}\left(\mathbf{p} - \frac{\hbar\omega}{\mathbf{v}_0}\right) + \rho^{(0)}\left(\mathbf{p} + \frac{\hbar\omega}{\mathbf{v}_0}\right) \right), \quad \text{where } \Upsilon = eE_c L / 4\hbar\omega$$

and we ignore the spontaneous contribution to the emission term with the approximation  $\nu_0 + 1 \approx \nu_0$ . The last two scattering terms represent symmetric photon-sideband spaced by  $\hbar\omega/\nu_0$  on both sides of the central momentum  $\mathbf{p}_0$  of the wavepacket as displayed in Fig. 2e. This quantum measurement result is similar to the measured electron energy gain/loss spectrum in PINEM experiments, in which the high-order sidebands were observed relating to multiple-photon emission and absorption processes [1-2].

For the Fock state of the photon system, the phase-dependent interference terms disappear due to the orthogonality of Fock states ( $\langle \nu_0 | \nu_0 \pm 1 \rangle = 0$ ) and thus lead to the same final projective momentum distribution as the measurement in the plane-wave limit, regardless of the electron's wavefunction profile corresponding to the classical or quantum limit. For the other three electron-photon couplings in Fig. 1c-e, either quantum electron or quantum photon corresponds to the final projective momentum distribution with no net momentum transfer  $\Delta\mathbf{p} = \int \rho^{(f)}(\mathbf{p})\mathbf{p}d\mathbf{p} = 0$  (i.e.,  $\Delta E = 0$ ), which implies no classical measurement for these three system-pointer interaction configurations.

**Is the classical acceleration a weak value?** As demonstrated in Figs. 2b,d, we find that the projective measurement [7] corresponds to the electron spectrum with discrete photon-sidebands of PINEM, and the weak measurement [8] to the accelerated spectrum with central momentum

shift. Moreover, the energy/momentum transfer is proportional to the classical electric field given by  $\mathbf{E} = -\langle \partial \hat{\mathbf{A}} / \partial t \rangle$ . Thus, we show that the classical point-particle acceleration is an effective weak value of the vector potential, i.e.,

$$\Delta \mathbf{p}_{\text{point}} \propto \mathbf{A}_w \equiv \frac{\langle \beta, \nu' | \hat{\mathbf{A}} | \alpha, \nu \rangle}{\langle \beta, \nu' | \alpha, \nu \rangle}, \quad (4)$$

where the pre- and post-selected photon states are defined as photon-added coherent states (1). Note that this definition of the vector-potential's weak value is applicable only if there is no time evolution of the photon system (except for the measurement process), or effectively, in short-time interaction. Two typical examples are considered with fixing the pre-selection and post-selection at the 'classical' or 'quantum' photon state:  $|\alpha, \nu\rangle = |\sqrt{\nu_0}, 0\rangle, |\beta, \nu'\rangle = |\sqrt{\nu_0}, 0\rangle$  (Figs. 1b,c);  $|\alpha, \nu\rangle = |0, \nu_0\rangle, |\beta, \nu'\rangle = |0, \nu_0\rangle$  (Figs. 1d,e). Also, these examples correspond to the electron energy transfers (i.e., Eq. 2) as we discussed in the previous two sections.

Now we describe the electron coupling process with classical-like photon system in the scheme of weak measurement [8,14], which is given by

$$\begin{aligned} & \underbrace{\langle \beta |}_{\text{post-selection}} \underbrace{\exp\left(-i \frac{1}{\hbar} \int_0^{L/v_0} H_1(t) dt\right)}_{\text{electron-photon coupling}} \underbrace{|\alpha\rangle \otimes |\psi(z)\rangle}_{\text{pre-selection}} \\ &= \langle \beta | \left( 1 + \left( \frac{ie}{\gamma_0 m \hbar} \right) \int_0^{L/v_0} (\hat{\mathbf{A}} \cdot \mathbf{p}) dt \right) |\alpha\rangle \otimes |\psi(z)\rangle \\ &= e^{-|\beta-\alpha|^2/2} \left| \psi \left( z + \left( \frac{e}{\gamma_0 m} \right) \int_0^{L/v_0} \mathbf{A}_w(t) dt \right) \right\rangle, \end{aligned}$$

where we employed the Coulomb gauge  $\nabla \cdot \hat{\mathbf{A}} = 0$ , the relation  $\langle \beta | \alpha \rangle = e^{-|\beta-\alpha|^2/2}$  for photon coherent states with real numbers  $\alpha, \beta$  and the short-time approximation  $L/v_0 \ll 1$ . The measuring electron pointer is assumed to be a Gaussian wavepacket in coordinate space ( $z$ )

corresponding to its momentum component (Eq. 1, i.e.,  $|\Psi\rangle$ ). The final spatial shift of the electron pointer is thus  $\Delta z = -(e/\gamma_0 m) \int_0^{L/v_0} A_w(t) dt$ , and the electron momentum transfer is approximated as  $\Delta p = \gamma_0 m (\Delta z / (L / v_0)) = -e (v_0 / L) \int_0^{L/v_0} A_w(t) dt = -e \bar{A}_w$ , which confirms the equivalence between the quantum wavepacket momentum transfer in the point-particle limit  $\Gamma \rightarrow 0$  and the time-averaged weak value of vector potential in the short interaction time approximation.

Let us discuss the post-selection of the final electron-photon states after interaction. Two types of ‘weak-valued’ electron-photon couplings are schematically shown in Fig. 3. In the reciprocal system-pointer setup of light-matter interaction, the electron can be the measured system and the photon is then the measuring pointer. If we are able to pre- and post-select the electron wavefunction, detection of the photon radiation rate ( $\Delta v$ ) then leads to a shift of the photon pointer, being the measuring pointer, as compared to the measurement of the momentum operator of the electron. In a recent work [10], the reciprocal relation between photon radiation and electron acceleration is demonstrated to be  $\Delta v + \Delta E / \hbar \omega = 0$ , which brings a correspondence between electron spectrum and photon spectrum that conserves the photon exchange in all measurement schemes. This ‘Acceleration/Radiation Correspondence’ (ARC) relation [10], connects the final measurements of the photon and electron spectrum with/without post-selection as a demonstration of the ‘system-pointer’ dualism. This setup of weak measurements resembles the pre- and post-selection of atomic states coupled with photons as proposed recently by Aharonov *et al.* [14].

Note that our quantum-to-classical measurement theory is entirely different from the environment-induced decoherence program [15-18]. Decoherence theory, the ‘classicality’ of which emerges from the natural loss of quantum interference by ‘leakage’ into the environment [17], misses the contributions of quantum interference, and would neither yield wavepacket-dependent acceleration nor periodic density bunching in the attosecond scale as in [9-10, 19-21]. Likewise, the environment-induced decoherence cannot produce the classical linear particle acceleration.

**Conclusion.** Four kinds of measurement setups in the context of electron-photon interactions were considered in detail, loosely corresponding to ‘classical electron’ and ‘classical photon’, ‘classical electron’ and ‘quantum photon’, ‘quantum electron’ and ‘classical photon’, and ‘quantum electron’

and ‘quantum photon’. We captured all these interaction types using our unified framework of measurement transition theory, defining all the physics above as a consequence of quantum weak measurement or quantum projective measurement. Then, the transition process was characterized by a universal factor  $e^{-\Gamma^2/2}$ , which could quantitatively verify our measurement theory in any experiment exhibiting light-matter interactions. Furthermore, our work reveals the continuous transition from weak to projective measurements, which can also explain the quantum-to-classical transition in common schemes like DLA and PINEM [13].

In addition, we identified the classical linear point-particle acceleration as the weak value of the vector potential, and connected it with the appearance of ‘classicality’ in quantum mechanics. This indicates that weak measurements not only reveal ‘anomalous’ quantum features of quantum physics, but also surprisingly describes classical characteristics in the realm of classical electrodynamics. The weak value of the vector potential under suitable pre- and post-selections offers a compelling theoretical framework for investigating the interaction between electron wavefunctions and quantum light sources such as superposition of Fock states, or squeezed states of light. In a subsequent paper [22] we further consider, both theoretically and experimentally, the weak-to-strong transition of quantum measurements in trapped ions as a consistent extension of our framework to generic system-pointer interactions.

### **Acknowledgements**

We wish to thank Eilon Poem for helpful discussions and comments. The work was supported in part. by Canada Research Chair and Ontario’s Early Researcher Award, by DIP (German-Israeli Project Cooperation), by I-CORE— Israel Center of Research Excellence program of the ISF, and by the Crown Photonics Center.

### **Competing financial interests**

The authors declare no competing financial interests.

## References

1. Feist, A., Echtenkamp, K. E., Schauss, J., Yalunin, S. V., Schfer, S. & Ropers, C. (2015). Quantum coherent optical phase modulation in an ultrafast transmission electron microscope. *Nature* 521, 200-203.
2. Barwick, B., Flannigan, D. J., & Zewail, A. H. (2009). Photon-induced near-field electron microscopy. *Nature* 462, 902-906.
3. Peralta, E. A., Soong, K., England, R. J., Colby, E. R., Wu, Z., Montazeri, B., & Sozer, E. B. (2013). Demonstration of electron acceleration in a laser-driven dielectric microstructure. *Nature* 503, 91-94.
4. Breuer, J., & Hommelhoff, P. (2013). Laser-based acceleration of nonrelativistic electrons at a dielectric structure. *Phys. Rev. Lett.* 111, 134803.
5. Zavatta, A., Viciani, S., & Bellini, M. (2004). Quantum-to-classical transition with single-photon-added coherent states of light. *Science* 306, 660.
6. Agarwal, G. S., & Tara, K. (1991). Nonclassical properties of states generated by the excitations on a coherent state. *Phys. Rev. A* 43, 492.
7. Von Neumann, J. (2018). Mathematical foundations of quantum mechanics: New edition. Princeton university press.
8. Aharonov, Y., Albert, D. Z., & Vaidman, L. (1988). How the result of a measurement of a component of the spin of a spin-1/2 particle can turn out to be 100. *Phys. Rev. Lett.* 60, 1351.
9. Gover, A. & Pan, Y. (2018). Dimension-dependent stimulated radiative interaction of a single electron quantum wavepacket. *Phys. Lett. A* 382, 1550-1555.
10. Pan, Y. and Gover, A., (2019). Spontaneous and stimulated emissions of a preformed quantum free-electron wave function. *Phys. Rev. A*, 99(5), 052107.
11. A. Friedman, A. Gover, G. Kurizki, S. Ruschin, and A. Yariv, (1988). Spontaneous and stimulated emission from quasi free electrons. *Rev. Mod. Phys.* 60, 471.
12. Kaminer, I., *et al.* (2016). Quantum Čerenkov radiation: spectral cutoffs and the role of spin and orbital angular momentum. *Phys. Rev. X* 6, 011006.
13. Pan, Y., Zhang, B. and Gover, A., (2019). Anomalous Photon-induced Near-field Electron Microscopy. *Phys. Rev. Lett.* 122(18), 183204.

14. Aharonov Y, Cohen E, Carmi A, Elitzur A. C. (2018). Extraordinary interactions between light and matter determined by anomalous weak values. *Proc. R. Soc. A* 474, 20180030.
15. Schlosshauer, M. (2014). The quantum-to-classical transition and decoherence. *arXiv preprint arXiv:1404.2635*.
16. Schlosshauer, M. (2005). Decoherence, the measurement problem, and interpretations of quantum mechanics. *Rev. Mod. Phys.* 76, 1267.
17. Zurek, W. H. (1992). The environment, decoherence, and the transition from quantum to classical. In *Quantum Gravity and Cosmology-Proceedings of The XXII Gift International Seminar on Theoretical Physics*, p. 117. World Scientific.
18. Bouchard, F., Harris, J., Mand, H., Bent, N., Santamato, E., Boyd, R. W., & Karimi, E. (2015). Observation of quantum recoherence of photons by spatial propagation. *Sci. Rep.* 5, 15330.
19. Priebe, K. E., Rathje, C., Yalunin, S. V., Hohage, T., Feist, A., Schäfer, S., & Ropers, C. (2017). Attosecond electron pulse trains and quantum state reconstruction in ultrafast transmission electron microscopy. *Nat. Photonics* 11, 793.
20. Kozák, M., Schönenberger, N., & Hommelhoff, P. (2018). Ponderomotive generation and detection of attosecond free-electron pulse trains. *Phys. Rev. Lett.* 120, 103203.
21. Morimoto, Y., & Baum, P. (2018). Diffraction and microscopy with attosecond electron pulse trains. *Nat. Phys.* 14, 252.
22. Pan, Y., *et al.* Observation of the weak-to-strong transition of quantum measurement in trapped ions, forthcoming.

Figures:

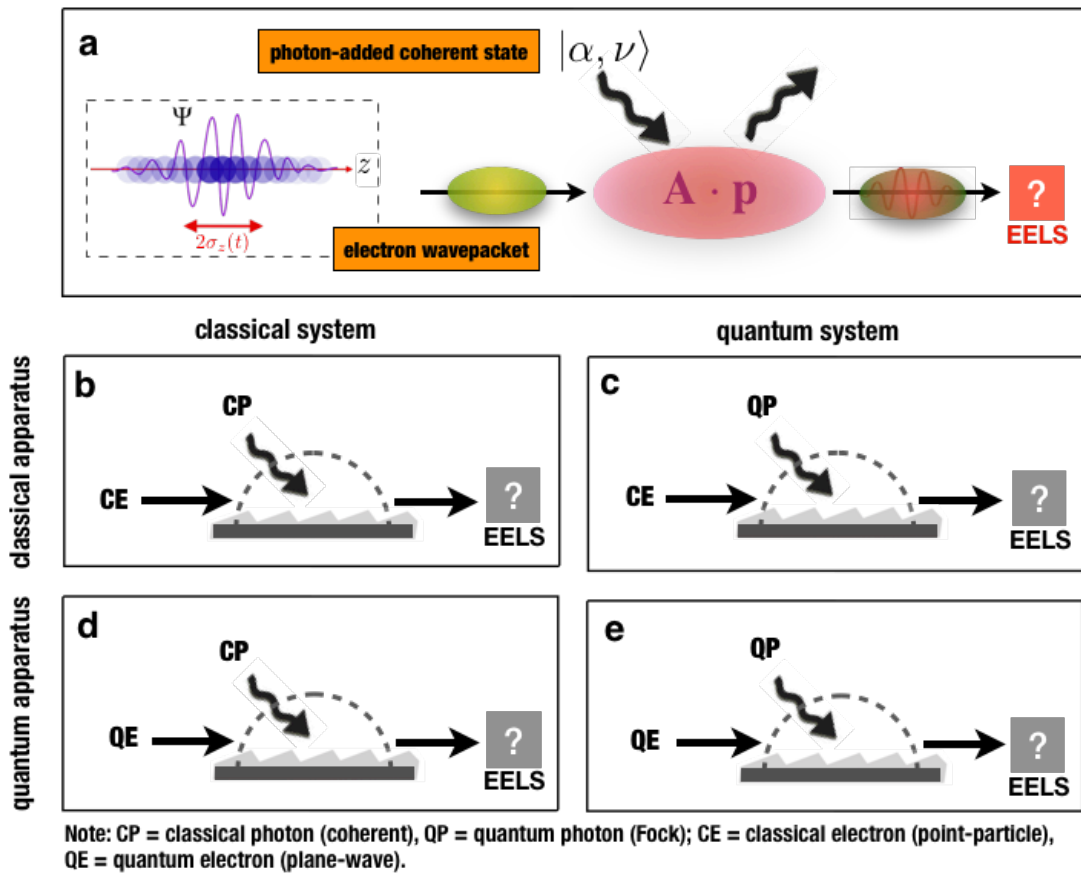


Figure 1 | The quantum and classical measurement schemes of the electron-photon interaction. (a) The classical photon (CP) in a coherent state and quantum photon (QP) in a Fock state are defined as two opposite limits of the photon-added coherent state  $|\alpha, \nu\rangle$ , where  $\nu = 0$  and  $\alpha = 0$  respectively. The classical electron (CE) and quantum electron (QE) are defined as the wavepacket representation in the point-particle limit and plane-wave limit, respectively (Eq. (1) in the text). The measuring pointer is the outgoing electron and the system is the pre-prepared photon state (without post-selection), with a coupling strength  $g$  between the system and pointer. (b-e) Four combinations of electron and photon interactions are presented in the classical and quantum measurement regimes. The readout of the measuring pointer is the electron energy loss spectrum (EELS).

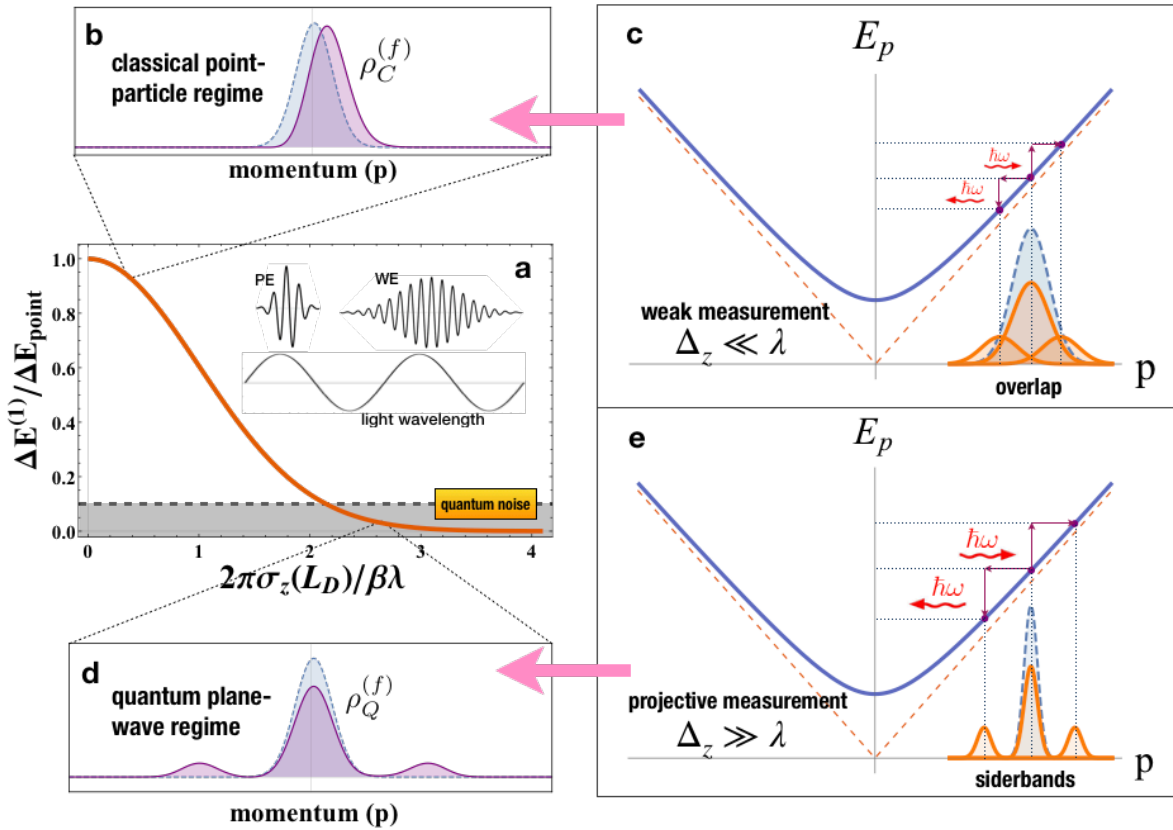


Figure 2| The quantum-to-classical measurement transition between the classical point-particle picture (b, c) and quantum plane-wave picture (d, e) of electron wavepacket pointer when coupled to a photon coherent state. The two limits of particle-like (b) and wave-like (d) pictures of the electron pointer in light-matter interaction corresponds to the classical (weak) measurement (particle acceleration) and quantum (projective) measurement (PINEM), respectively. The exact expressions of the final electron momentum distributions are presented in the text.

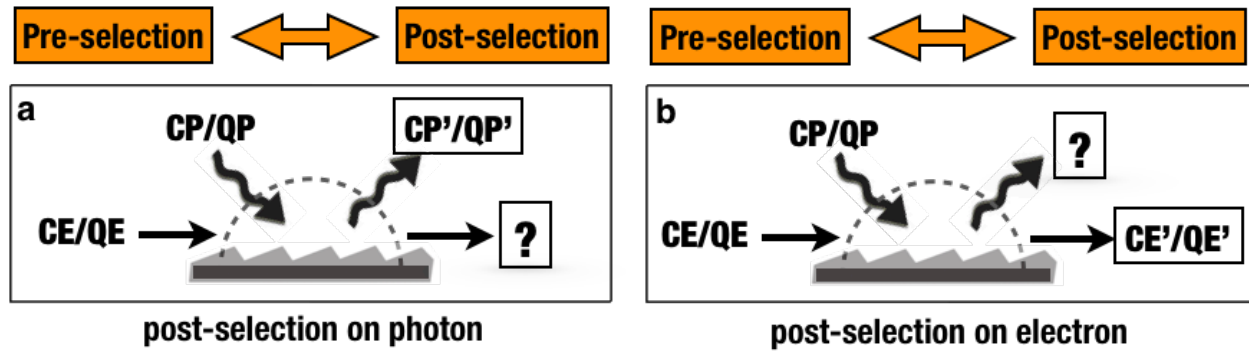


Figure 3| The weak-valued electron-photon interaction with pre-/post-selection on photons (CP/QP) and electrons (CE/QE), respectively. The pre- and post-selection are performed on (a) the photons or (b) the electrons as the measured system, and the rest acts as the measuring pointer in quantum-to-classical measurement schemes.